Electronic Monitoring of Events within Dynamic Particulate Beds: Conductance and Capacitance Measurements

EDWARD G. RIPPIE ×, DOUGLAS C. KRIESEL *, and HARALD RETTIG ‡

Received July 15, 1976, from the *Department of Pharmaceutics, College of Pharmacy, University of Minnesota, Minneapolis, MN 55455.* Accepted for publication November 15, 1977. *Present address: Abbott Laboratories, North Chicago, IL 60064. ‡Present address: Ciba-Geigy Corp., Basel, Switzerland.

Abstract □ Methods for monitoring mechanical events occurring within particulate solids systems in a dynamic state are described. The electrical conductance and capacitance characteristics of such systems, as they relate to the degree of bed dilation or expansion, extent of interparticulate contact, and intensity of particle motion, were studied and are discussed. To establish the potential of this approach, harmonically vibrated beds of monodispersed conducting spheres were used. A technique, based on the frequency modulation of standard FM broadcast frequency carrier signals, was developed to measure low and high frequency fluctuations in bed capacitance. The electrical conductance of these systems also was determined by both voltage drop and current flow methods. The experimental techniques developed are broadly applicable to various materials and modes of agitation or flow. They permit the evaluation of the time courses of both bed dilation and particle motion which, in turn, are known to determine or modify critically powder flow and mixing behavior.

Keyphrases □ Particulate beds, dynamic—electronic monitoring of mechanical events, conductance and capacitance characteristics evaluated □ Solids—dynamic particulate beds, electronic monitoring of mechanical events, conductance and capacitance characteristics evaluated □ Electronic monitoring—mechanical events in dynamic particulate beds, conductance and capacitance characteristics evaluated

Solids mixing research has concentrated on the development of experimental methodology and the elucidation of the underlying mechanisms responsible for the mixing and segregation characteristics of multiparticulate solids systems (1–4). From these mixing studies at the particulate level, it became evident that much new information could be gained from the quantification of certain fundamental properties of dynamic particle beds. Two kinematic properties in particular that seemed of value to characterize were generalized bed dilation and individual particulate motion. These properties result whenever adjacent regions of a free-flowing multiparticulate system are caused to move relative to each other. This movement occurs when vibration or shear is induced by mixing operations or by processes in which noncohesive powders are made to flow.

An understanding of the extent and time course of bed dilation is important. Both the degree of interparticulate contact and the associated magnitude of the energy barriers that individual particles must overcome in moving past each other are strongly dilation dependent. Moreover, measurements of the intensity of particle motion within a particulate bed provide evidence of the relative kinetic energy content of the particles and their patterns of energy decay through energy-absorbing collisions, particle attrition, and other kinetic energy-consuming interparticulate interactions.

For particles to move past each other without fracturing, they not only require space in which to move but also must possess the energy necessary to overcome interparticulate frictional forces. Because the average particle kinetic energy and the associated degree of bed dilation are frequently strongly coupled, these quantities ideally should be measured simultaneously by techniques that do not perturb the system. Such techniques will be most useful if they possess the following characteristics: a wide range of application capable of providing data on beds having varied particulate compositions and subjected to vibration and/or shear, the ability to detect rapidly occurring changes of very short duration throughout the bulk of a given particulate system, and a high degree of sensitivity to small relative changes in bed characteristics.

Furthermore, the response of any such measurement technique to rapid bed changes should be stable, reproducible, and flat over the range of approximately 20–15,000 Hz. This frequency range should cover adequately the frequency spectrum of events occurring within typical systems. Since, in vibrated beds, the degree of bed expansion and the intensity of particle motion are expected to be approximately periodic functions of time, corresponding to the periodicity of vibration, an ideal measurement technique should permit the resolution of events within the time base of a single vibratory cycle.

The characteristics described as being desirable for monitoring changes in void volume and particulate motion of dynamic multiparticulate solids systems were found in this study to be satisfactorily met by techniques for measurement of their electrical conductance and behavior in a capacitor. This paper describes the operational characteristics of these techniques and illustrates their utility and that of data acquired from vibrated beds of spherical conducting particles of uniform density.

DESIGN CONSIDERATIONS

A bed of electrically conducting particles can be visualized as a three-dimensional network of switches with interconnecting conductors. In a vibrated bed, these switches are constantly being opened and closed as the bed expands and contracts. The conductance is a function not only of the multiplicity of conducting pathways between sensing electrodes placed in such beds but also of the interparticulate contact pressures that determine virtual contact areas between particles and, hence, contact resistances. Changes in bed conductance can be observed from measurements both of voltage drops across the bed and of current flow through the bed under conditions of constant circuit voltage. Both approaches were used in the present studies.

The nature of the dependence of bed conductance on interparticulate contact, assuming any and all contacts are of low resistance, can be seen from a consideration of the probability of electrical continuity through a chain of n particles. If the probability of contact between any two adjacent particles in the chain is p, then the probability of chain conduction is p^{n-1}, provided end particles contact electrodes. In the systems studied, many paths of various lengths (numbers of particles) between the electrodes were possible.

It is characteristic of such systems that, for a fixed interelectrode distance, the number of possible paths of a given length increases as the path length increases. However, since for a given value of p, the probability of conduction per path drops rapidly with increased path length, only the shorter paths contribute significantly to conduction. Calculation of the number of paths as a function of their length was not possible because of random bed packings.

0022-3549/78/0800-1121$01.00/0

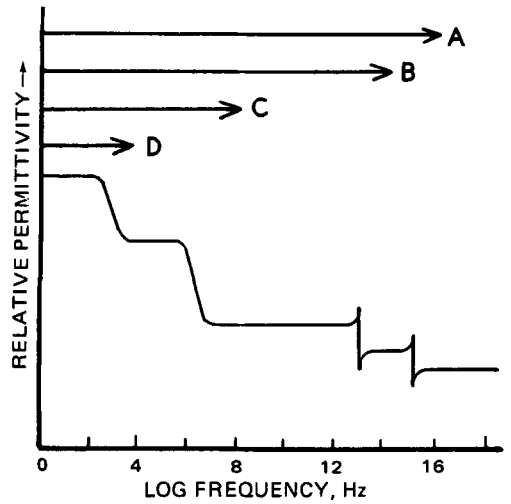

Figure 1—*Dependence of relative permittivity on frequency. Frequency ranges of the contributions to permittivity from electronic (A), atomic (B), dipole (C), and interfacial (D) sources are indicated.*

The probability of conduction through a typical path, 33 particles in length, decreases from 0.725 to 0.194 as p decreases from 0.99 to 0.95. With the probability of adjacent particle contact at 0.5, the probability of electrical continuity drops to 2.33×10^{-10}. Bed conductivity can be expected to reflect small changes in the degree of interparticulate contact when such contacts are highly probable. However, such measurements cannot be expected to reflect unambiguously bed packing densities since, for example, even a hexagonally close packed array of conducting spheres will be nonconducting if uniformly expanded by a minuscule amount.

Consider next the capacitance, C, of a parallel plate condenser which, by definition, is directly proportional to the relative permittivity, ϵ', of a dielectric material placed between the plates (5), as can be seen from:

$$C = \frac{\epsilon_0 \epsilon' A}{d} \qquad \text{(Eq. 1)}$$

where A is the plate area and d is the distance of separation between the plates. Capacitance changes resulting from short- and long-term permittivity changes of liquids, liquid suspensions, and gas–solid mixtures have been determined with the aid of microwave resonance chambers, capacitance bridges, and oscillating circuits (6–9). In contrast, very small, high frequency changes in capacitance were anticipated to occur in the present systems because of changes in the effective distance of separation of the plates, d, rather than changes in permittivity as such. The effective thickness of air separating the plates fluctuates because of changes in the spatial configuration and number of conducting spheres between the plates.

An electric oscillator in its simplest form consists of an inductance coil and a condenser connected end to end. Power losses due to resistance or radiation are compensated by a suitable driving circuit so as to maintain oscillation. The resonant frequency, f, of an electronic oscillator is a function of the capacitance, C, and is given by the expression (10):

$$f = \frac{1}{2\pi\sqrt{LC}} \qquad \text{(Eq. 2)}$$

where L is the inductance. By coupling a capacitor, having the particle bed as its dielectric, into such a circuit, the previously listed design requirements would be met. With the circuit tuned to a nominal frequency of several megahertz, small changes in bed configuration or packing density would result in substantial frequency changes that could be measured accurately. Moreover, rapid changes in capacitance would be readily detectable since the bed would be scanned several million times per second.

Care must be taken, however, when selecting the mean frequency since the permittivities of static dielectrics, air and the container in this case, are a function of frequency (Fig. 1). A frequency of 100 MHz was selected since it falls within both a frequency-independent permittivity region and the commercial FM broadcast band. Relatively inexpensive transmitting and receiving equipment capable of excellent response characteristics is available and can easily be adapted for these studies.

A parallel plate condenser was constructed with plates of a length and width so that a well-defined segment of the bed constituted a major portion of its dielectric medium.

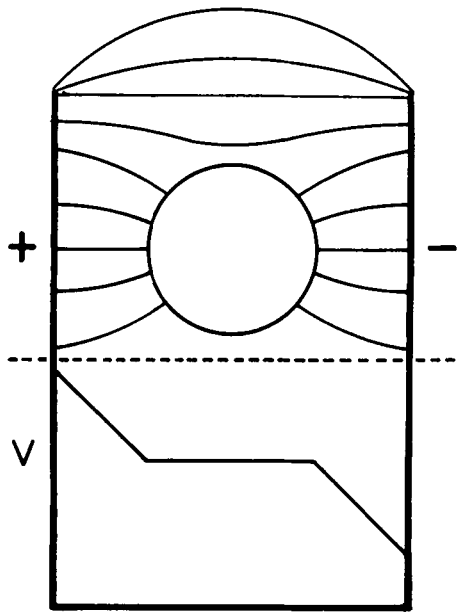

Figure 2—*Top: electrical field pattern for a conducting sphere between two parallel condenser plates. Bottom: potential drop through the center of the sphere and to the surfaces of the plates.*

Figure 2 illustrates the effects of a single spherical conducting particle on the electric field between parallel capacitor plates. The instantaneous effect, at a given time, of a dynamic bed of conducting particles on an otherwise uniform external electric field is vastly more complex. Assuming no electrical contact between conducting spheres comprising the bed, successful theoretical treatments of apparent permittivity are limited to solid–gas volume ratios of 0.25 and less (11). Since the volume fraction of solids in the present systems was estimated to range from approximately 0.5 to 0.7, calculation of capacitance was not feasible.

Further complications arise since interparticulate contacts lead to increased capacitance *via* networks of touching particles. Such clusters behave, in effect, as individual conducting particles of various sizes and configurations. Thus, each particle or electrically connected cluster of particles lying within the condenser alters the electrical field. Changes in bulk density due to bed dilation and changes in the electrically connected clusters due to particle motion, in combination, elicit changes in the effective thickness of the dielectric separating the plates and consequently produce corresponding capacitance changes.

As has been indicated, capacitance changes within an oscillating circuit result in a frequency modulated signal. This signal can be demodulated by an FM detector in standard fashion to yield a signal whose amplitude is proportional to the frequency shift and whose frequency corresponds to the rate (frequency) of modulation of the carrier frequency. Consider a carrier signal having a peak-to-peak amplitude of $2A$ and a phase angle as a function of time, t, as given by θ. The amplitude of the signal, y, is given by (12):

$$y = A \sin\theta = A \sin(\omega_0 t + \varphi) \qquad \text{(Eq. 3)}$$

$$\varphi = \alpha \int_{-\infty}^{t} m(t)\, dt \qquad \text{(Eq. 4)}$$

where ω_0 corresponds to the angular velocity of the electrical vector of the unmodulated carrier. A shift, φ, in phase angle is proportional to the time integral of a modulating signal, $m(t)$, through a constant, α, as shown in Eq. 4. The carrier frequency, f_0, and the instantaneous frequency, f, at any time, t, are given by the following relationships:

$$2\pi f = d\theta/dt = \omega_0 + d\varphi/dt \qquad \text{(Eq. 5)}$$

$$2\pi f_0 = \omega_0 \qquad \text{(Eq. 6)}$$

Thus, combining Eqs. 5 and 6 gives:

$$2\pi(f - f_0) = d\varphi/dt \qquad \text{(Eq. 7)}$$

Differentiating Eq. 2 with respect to capacitance yields:

$$\frac{df}{dC} = \frac{-C^{-3/2}}{4\pi L^{1/2}} \qquad \text{(Eq. 8)}$$

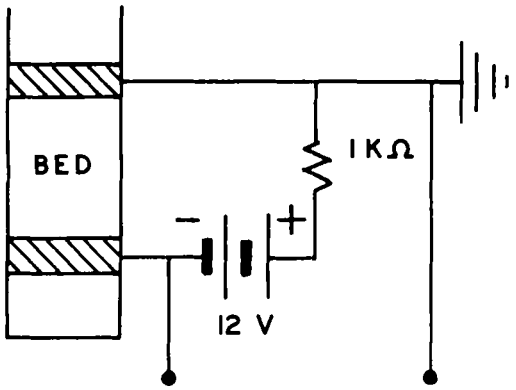

Figure 3—*Electrical circuit used for measurements of both bed voltage drop and conductance.*

If changes in capacitance are small in comparison with total capacitance, Eq. 8 reduces to:

$$\Delta f \cong -K\,\Delta C \qquad \text{(Eq. 9)}$$

where K is a proportionality constant. This condition is satisfied in commercial FM transmission and was valid in the present work.

Combining Eqs. 7 and 9 yields:

$$d\varphi/dt = 2\pi\,\Delta f = -2\pi K\,\Delta C \qquad \text{(Eq. 10)}$$

Integration of Eq. 10 and substitution into Eq. 4 yield the following relationship between capacitance changes and the nature of the modulating signal:

$$\int_{-\infty}^{t} m(t)\,dt \cong -(2\pi K/\alpha)\int_{-\infty}^{t} \Delta C\,dt \qquad \text{(Eq. 11)}$$

Thus, there is a direct relationship between changes in capacitance and the "audio" output of the FM receiver. The demodulation of the carrier signal, having a frequency modulated by the coupled bed capacitor, permits an unambiguous measurement of changes in relative capacitance.

EXPERIMENTAL

Materials and Equipment—A mechanical shaker, designed to generate nearly pure sinusoidal motion, provided the energy input into the particle beds. Previous studies (1–4) were conducted with this equipment and mode of agitation. In this study, the shaker frequency was held at 17.09 Hz while peak-to-peak amplitudes were varied from 0.254 to 0.508 cm.

A 2.54-cm i.d. segmented polycarbonate[1] tube, 20 cm long, was used as the bed container for the conductivity measurements. Segments were 1.6 cm in length; two were brass and served as electrodes. The particulate bed was approximately 12 cm deep, and the electrodes were centered 7.2 and 2.4 cm from the bottom of the bed. Capacitance experiments were conducted on beds of the same depth in 2.54- and 3.18-cm i.d. acrylic[2] tubes, 40 cm long. These tubes were fitted with plungers from the bottom capable of moving the particle bed vertically to position various bed regions within the sensing zone of the capacitor.

The parallel plate capacitor consisted of two copper sheets (1.5 × 7.5 cm) mounted 4.7 cm apart on a rectangular block of acrylic. The block had a central bore, allowing it to be positioned around the cylinder containing the bed. The monodispersed particle beds consisted of 304 g of chrome steel spheres[3], ranging from 0.238 to 0.556 cm in diameter.

Conductance and Capacitance Circuits—Conductance measurements were made using the circuit depicted in Fig. 3. A 12-v dc potential was placed across the bed with a 1-kohm resistor in series. The voltage drop across the bed was measured using a high impedance probe[4] through the dual-trace amplifier[5] of a 50-MHz oscilloscope[6] with a 7-nsec rise time. The probe was connected between the negative pole of the voltage supply and the bed, with the ground connector at ground potential as

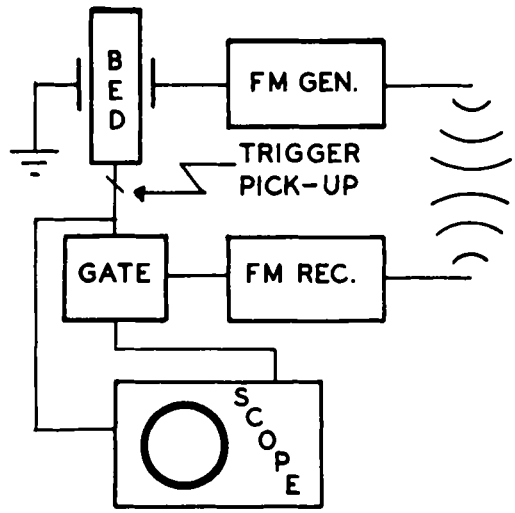

Figure 4—*Block diagram of circuit used for measurements of the particle bed relative capacitance.*

shown in Fig. 3. Current flow measurements were made on the same circuit as was used for voltage drop determinations, using an ac current probe[7] with a current flow amplifier[8]. The probe was placed over the conductor between the 1-kohm resistor and the positive pole of the power supply.

The circuitry employed to monitor capacitance changes is represented by Fig. 4. The bed condenser plates were extended horizontally beyond the diameter of the cylindrical bed container to minimize fringe effects. Acquisition of stray capacitance contributions from the mixer was avoided by placing a grounded aluminum shield in the proximity of the capacitor, isolating it from the shaker. The shield, capacitor, and bed container were mechanically connected and moved together with the same amplitude and frequency.

One plate of the capacitor was grounded, and the other was connected in parallel to the carrier oscillator of an FM transmitter[9]. The carrier frequency was tuned to approximately 100 MHz and broadcast. It was received by a standard FM radio ratio–detector receiver[10]. The resultant "audio" frequency output from the receiver was fed through a gating circuit (Fig. 5; see *Appendix*) and displayed on the oscilloscope. A magnetic pickup coupled with a magnet mounted on and revolving with the shaker flywheel provided a voltage pulse that served as a trigger signal for the oscilloscope and the gating circuit. This arrangement permitted the correspondence between the signal output and the shaker phase angle

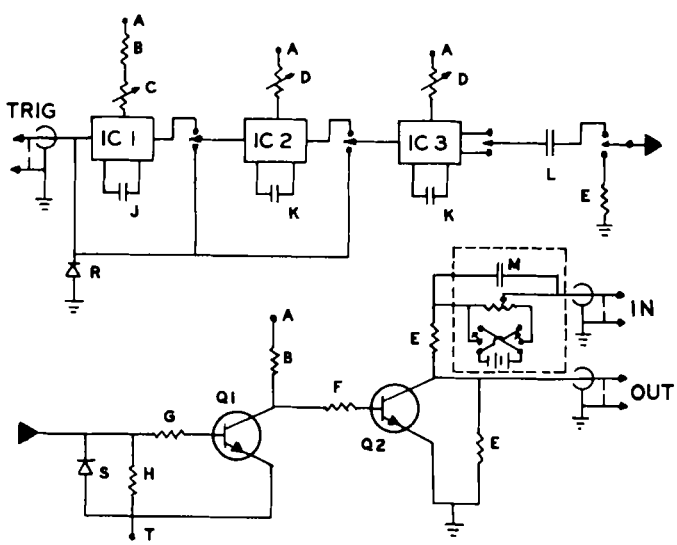

Figure 5—*Circuit diagram of the time delay triggered gate having a wide band frequency pass.*

[1] Lexan, General Electric Co.
[2] Lucite, du Pont.
[3] Atlas Ball Division, SKF Industries.
[4] P 6008 10X probe, Tektronix, Inc.
[5] Type 1A2 plug-in unit, Tektronix, Inc.
[6] Type 547, Tektronix, Inc.
[7] P 6021 current probe and termination, Tektronix, Inc.
[8] Type 134 current probe amplifier, Tektronix, Inc.
[9] Model 1G-37 FM stereo generator, Heath Co.
[10] Model AR-27 FM solid-state receiver, Heath Co.

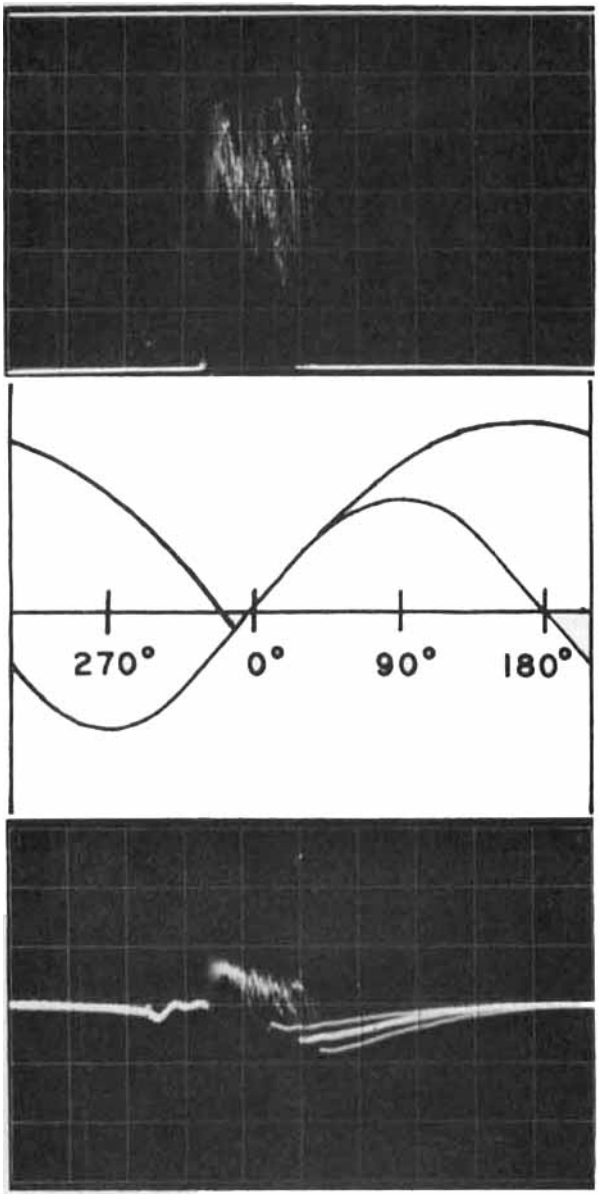

Figure 6—*Relationship of voltage drop (upper trace) and conductance (lower trace) to phase angles and projected free-flight behavior (center curve). Traces show eight cycles each of a bed composed of 0.397-cm diameter steel spheres shaken at a peak-to-peak amplitude of 0.442 cm. Sensitivities are −2 v/div and 1 mamp/div for the upper and lower traces, respectively.*

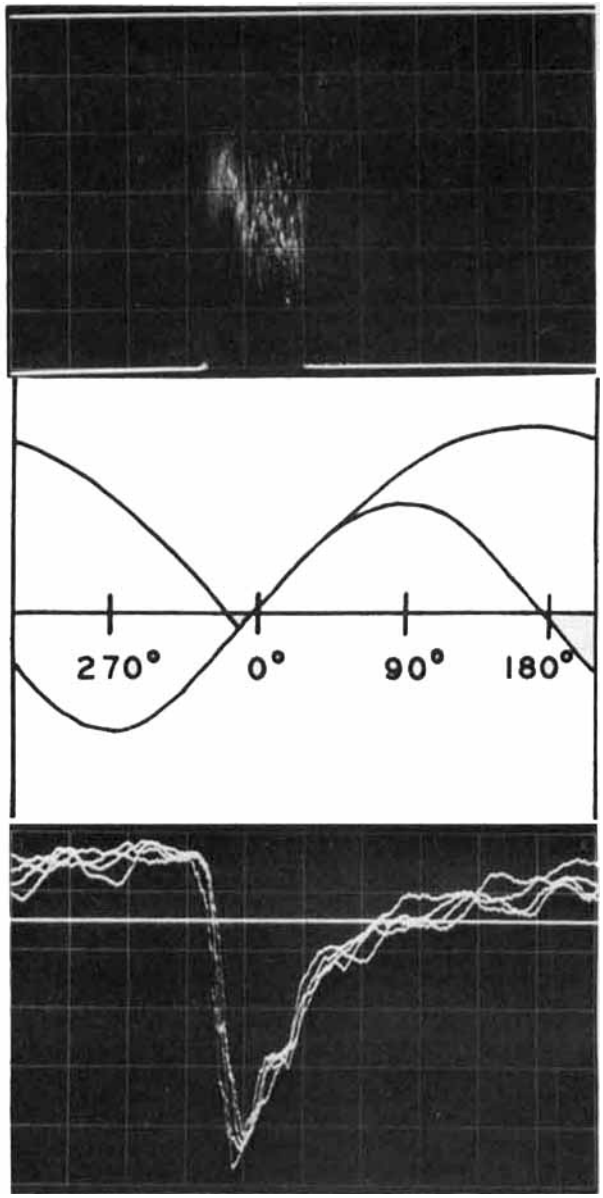

Figure 7—*Relationship of voltage drop (upper trace) and capacitance (lower trace) to phase angles and projected free-flight behavior (center curve). Traces show eight cycles each of a bed composed of 0.397-cm diameter steel spheres shaken at a peak-to-peak amplitude of 0.442 cm. Sensitivities are −2 v/div and 50 mv/div for the upper and lower traces, respectively.*

to be determined. The flywheel was calibrated so that the trigger magnet could be adjusted to produce a voltage pulse at any desired shaker phase angle.

FM receiver output signals were displayed as amplitude *versus* time after suitable amplification or were fed into a spectrum analyzer[11] and displayed on the scope as amplitude *versus* frequency spectra over selected frequency ranges. The frequency spectrum of the signal generated through FM modulation changed continuously during each shaking cycle. For this reason, the gating circuit was designed to permit frequency analysis over selected time intervals of various duration during each cycle.

Signal Processing—Voltages produced during conductance studies were measured using the dual-trace amplifier to display simultaneously the trigger and bed voltage signals. The sweep time of the scope was calibrated so that the full width of the CRT graticule corresponded to one cycle of the shaker. Voltage fluctuations were then displayed at a vertical deflection of 100–200 mv/graticule division. Current flow measurements differed from this system only in that the ac current probe and current probe amplifier were used in place of the voltage probe.

As mentioned previously, bed capacitance was a function of time over the period of a shaking cycle. The FM output signal was observed to vary in voltage by relatively large amounts in cycles (17.09 Hz) corresponding to the frequency of the shaker and to contain relatively high frequency, low amplitude voltage fluctuations. The former signal features varied only slightly from cycle to cycle and were not analyzed for their frequency content.

The FM receiver was tuned to the 100-MHz carrier frequency of the transmitter, using a 1-kHz audio reference signal available in the stereo generator used for transmission. Following tuning, the reference signal was turned off and shaking was begun. Observed audio outputs were thus solely due to fluctuations in capacitance due to the bed. With an open gate, calibration of the graticule was carried out to portray one cycle of agitation in the same manner as described for conductance measurements. All measurements were made with the capacitor centered 5 cm above the bottom of the particle bed.

Higher frequency components of the FM output signal (100 Hz–10 kHz) were examined over the entire agitation cycle. Measurements were

[11] Type 1L5, Tektronix, Inc.

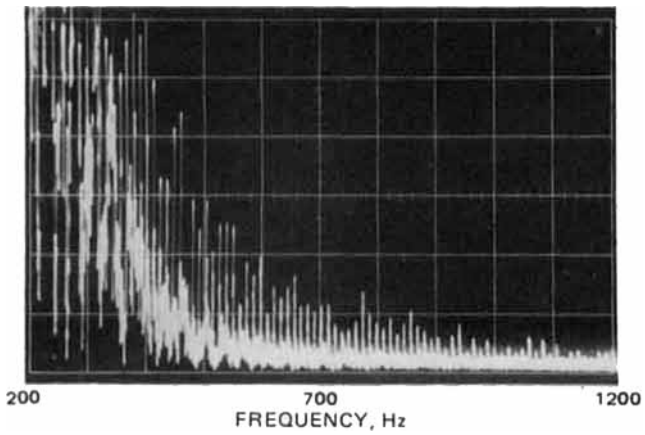

Figure 8—*Spectrum of capacitance changes over the frequency range of 200–1200 Hz. The bed was composed of 0.397-cm diameter steel spheres shaken at a peak-to-peak amplitude of 0.442 cm. Sensitivity is 0.4 v/div.*

made by two procedures. In the first, the spectrum analyzer was set to scan continuously from low to high frequency at rates of 100–200 Hz/sec with a dispersion of 100 Hz/horizontal scale division. Therefore, a single sweep of the CRT beam across the 10 divisions of the graticule provided a frequency scan over a range of 1 kHz. The interval of 200–1200 Hz was selected as being characteristic of this general frequency range, since signal amplitudes were very low above this range.

The second procedure for spectrum analysis was designed to provide information over limited agitation phase intervals and was a modification of the method described for full cycle scans. The gate was set to open for a predetermined 36° interval during each shaking cycle and to pass no signal during the remaining fraction of the cycle. A highpass filter[12] was inserted into the circuit between the FM receiver and the oscilloscope. This filter removed frequencies below 100 Hz and served to eliminate difference frequencies originating with the 17-Hz chopping action of the gate. As before, the spectrum analyzer was set to scan from 200 to 1200 Hz, providing spectral information on the cycle time segment selected. This procedure was used successively to examine piecewise the full shaking cycle. Intensity was displayed as root mean square (rms) voltage at a given frequency, and the spectrum analyzer was frequency and amplitude calibrated using a signal generator[13] and a frequency counter[14].

Conductance and capacitance measurements were recorded on high contrast film[15] using an optically projected graticule. Exposures were made of both single and multiple scans, some of which are included in Figs. 6–9.

RESULTS AND DISCUSSION

The concept of the free-flight trajectory of a nonrebounding particle subjected to vertical harmonic shaking is useful as an idealized model in considering the motion of a particulate bed subjected to a similar agitation (3, 13, 14). In this model, the hypothetical nonrebounding particle follows the vertical sinusoidal motion of the shaker until the downward acceleration of the shaker exceeds that of gravity. At this point, the particle lifts free and follows a free-flight vertical trajectory until it again contacts the shaker. This behavior is illustrated in Fig. 10, which depicts the free-flight trajectories for particles subjected to the same amplitudes as the particle beds under investigation. For comparison, the individual trajectories are drawn to the scale of a single shaker amplitude. Peak-to-peak agitation amplitudes of 0.254, 0.358, 0.442, and 0.508 cm were sufficiently low that bed liftoff and landing fell within a single cycle.

One can obtain an approximate view of general bed behavior by analyzing various periods of the free-flight trajectory. After takeoff, the bed expands rapidly; it then remains more or less in a uniformly expanded state. As the shaker begins its upward movement, the bed quickly collapses and is caught up by the ascending base of the chamber. The actual time required for maximal bed compression also depends on the rate of

[12] Model F 250, Allen Avionics Co.
[13] Model 144 HF sweep generator, Wavetek Co.
[14] Model 390 digital multimeter, Anaconic, Inc.
[15] Type 127, Polaroid.

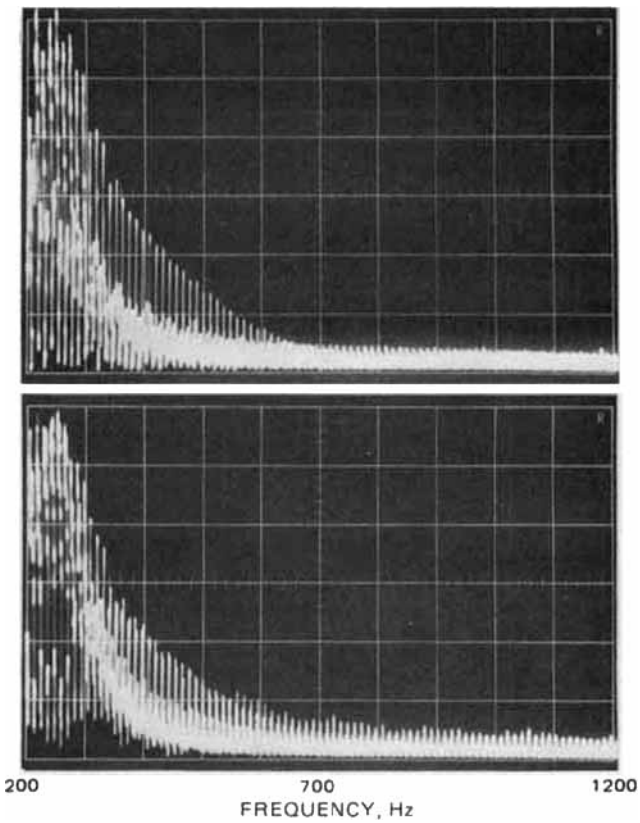

Figure 9—*Spectra of capacitance changes over the frequency range of 200–1200 Hz for 36° phase intervals. Phase intervals are 65–101° for the upper trace and 245–281° for the lower trace, and sensitivities are 50 and 80 mv/div, respectively.*

kinetic energy decay by frictional, intraparticulate acoustic, and other losses. The minimum porosity, corresponding to maximal compression, exists only for an instant during each cycle.

The relationship of voltage drop and current flow traces to the free-flight model is shown in Fig. 6. These tracings indicate the period during which the bed is conducting. Amplification settings were chosen for convenient display. Baseline distortion of the lower trace is an artifact from the current probe. Loss of conduction coincides with the expected time at which bed expansion begins, and its reestablishment occurs near the expected time at which bed compression begins.

A preliminary series of measurements was made at various bed locations and indicated that the upper bed expanded first and was the last to be compressed, whereas the lower bed was expanded for the shortest period of time. This behavior is indicative of frictional wall effects, and measurements of its magnitude are of potential value in quantitating particle–wall interactions.

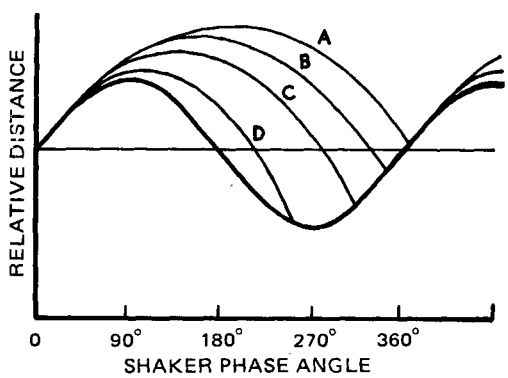

Figure 10—*Free-flight trajectories for a nonrebounding particle subjected to vertical harmonic shaking of various amplitudes. Trajectories are each drawn to the scale of the sine wave. Trajectories are shown for peak-to-peak shaker amplitudes of 0.508 (A), 0.442 (B), 0.358 (C), and 0.254 (D) cm.*

Table I—Shaking-Phase Angles of Bed Conductance Changes

Shaker Amplitude, cm	Sphere Diameter, cm	Phase Angle of Conduction, Ending/Onset	Relative Phase Angle[a] of Particle Bed, Liftoff/Landing
0.254	0.238	31°/262°	6°/−15°
	0.397	51°/239°	−14°/8°
	0.556	41°/254°	−5°/−7°
	0.635	41°/260°	−5°/−13°
0.358	0.238	32°/295°	−7°/9°
	0.397	48°/301°	−23°/3°
	0.556	33°/306°	−8°/−2°
	0.635	38°/306°	−13°/−2°
0.442	0.238	33°/311°	−12°/30°
	0.397	43°/309°	−22°/32°
	0.556	26°/327°	−4°/13°
	0.635	3°/341°	18°/0°
0.508	0.238	33°/353°	−16°/11°
	0.397	31°/357°	−13°/7°
	0.556	34°/344°	−17°/20°
	0.635	20°/348°	−3°/16°

[a] Phase angles of apparent bed liftoff and landing, based on measurements of bed conductance, expressed relative to liftoff and landing phase angles as predicted by free-flight calculations.

Table II—Shaking-Phase Angles of Characteristic Capacitance Changes of Particulate Beds

Shaker Amplitude, cm	Sphere Diameter, cm	Phase Angle at Which Slope Changes[a]	Phase Angle	
			Minimum Capacitance	Maximum Capacitance
0.254	0.238	44°	230°	274°
	0.397	53°	216°	275°
	0.556	37°	188°	270°
	0.635	45°	157°	271°
0.358	0.238	42°	303°	324°
	0.397	43°	272°	322°
	0.556	39°	284°	315°
	0.635	35°	223°	330°
0.442	0.238	35°	306°	353°
	0.397	44°	271°	352°
	0.556	45°	293°	347°
	0.635	40°	250°	322°
0.508	0.238	29°	341°	12°
	0.397	39°	325°	1°
	0.556	30°	326°	4°
	0.635	34°	310°	351°

[a] The phase angle at which the rate of decrease of capacitance decreases, resulting in a slope change in the curve and reflecting a change in bed behavior.

Shaker phase angles corresponding to the termination and onset of bed conductance are listed in Table I. The ascending neutral position of the shaker, midway between its lower and upper extremes of motion, is the designated reference point for phase angle measurements. This reference point is used for both Tables I and II and is the point during the upward motion of the shaker when its acceleration is zero. Identical data on this behavior were obtained from measurements of either amperage or voltage drop; however, voltage measurements were largely used because of the relative ease of reading the scope. Four monodispersed systems were examined at each agitation amplitude.

Column three in Table I consists of number pairs, the first number indicating the phase angle at which conduction was terminated and the second number indicating the angle where conduction was resumed. Thus, the interval between these angles was the time period during which the bed was in an expanded state sufficient to prevent conduction.

Column four in Table I also consists of number pairs, representing the differences in phase angles between measured and predicted bed liftoff and landing. For example, a "0" means that the measured (*via* conductance) and the predicted (*via* the free-flight model) phase angles were the same. If a drop in bed resistance appeared prior to the predicted time, it is indicated by a positive angle; conversely, negative angles signify delayed bed response times. In most cases, bed expansion began slightly later than predicted by the free-flight model. Bed contractions tended to begin earlier than predicted by the model; however, this result is not unexpected since a late liftoff would result in a lower projection velocity.

Figure 7 illustrates the relationships typically observed between the bed voltage drop and the FM receiver output in comparison with the free-flight model. Several features of these scans can be related to the dynamic behavior of the particle bed. The establishment of interparticulate contact, as evidenced by a marked decrease in bed resistance, occurred within the time period when capacitance was increasing abruptly. Keeping in mind the relationship expressed in Eq. 9, such an increase in capacitance would result in lowered carrier frequency and decreased receiver output voltage. This relationship is also dependent on the number of signal inversions occurring in the amplification stages in the receiver.

The phase relationship was established from the receiver circuit schematic and verified experimentally in this study. Consequently, negative FM output voltages signify increased capacitance, and the converse is true for positive signals. The point of greatest capacitance fell very close to the time of predicted complete bed collapse. The characteristic break in the slopes of the capacitance curves coincides closely with a loss of bed conductivity and the free-flight liftoff time. Capacitance decreases gradually to a minimum just before bed collapse begins.

To avoid signal distortions, it was essential that the response of the audio amplifier was linear over the frequency range of interest and, in particular, down to the 17-Hz frequency of the shaker. This response was verified experimentally to hold at the amplification levels employed.

These events are well correlated with the idealized free-flight behavior for the monodispersed system shown; however, segregation behavior of binary systems containing this size particle as the large component showed little or no wall effects (2). Where such effects do occur, predictions of bed behavior based on free-flight considerations are of little value, and measurements of relative bed conductance and capacitance as outlined are necessary. Phase angles corresponding to the times of minimum and maximum capacitance are listed in the last two columns of Table II for various shaker amplitudes and particle sizes. As stated earlier, changes in capacitance can result from either of two mechanisms: a change in the relative bed density or a change in the number or density of interparticulate contacts within the bed. Obviously, both mechanisms must be considered when the data are interpreted.

Decreasing capacitance, for example, can be due to bed expansion and/or loss of interparticulate contact. The lowest trace in Fig. 7 shows that the capacitance decreases in two stages: an initial rapid decrease followed by a more gradual decrease. This behavior is shown by the rising right-hand portion of the trace. The phase angle at which the rate of capacitance decrease changes (decreases) is listed in column three of Table II. The time of this change of slope is shown in Fig. 7 to correspond closely with the time at which conduction ceases, as previously indicated. The initial rapid decrease in capacitance was likely due to a reduction in both cluster size and bed density, while the slower capacitance drop was due primarily to a continuing decrease in bed density.

Before considering the implications of frequencies in the range of 200–1200 Hz in the FM audio signal, it is important to examine the operating characteristics of the spectrum analyzer. The analyzer used was of the real-time type, which performed a continuous frequency analysis of the incoming signal. This examination does not constitute a Fourier analysis but instead indicates the composition of the signal at a given time during the shaking cycle. This composition was verified experimentally by examining single frequency, sinusoidal signals pulsed at 17 Hz by the gate. As mentioned earlier, a highpass filter was used to eliminate the 17-Hz waveform from the signal prior to analysis and also served to eliminate difference frequencies that otherwise originated with the 17-Hz chopping action of the gate. Since the amplitude of these higher frequencies was substantially less than that of the 17-Hz waveform, they are not readily apparent in Fig. 7.

The presence of these higher frequency components in the FM receiver output signal is illustrated by the typical spectrum shown in Fig. 8. Each spike in the figure represents the amplitude–time relationship over the period of a single shaking cycle. The frequency being scanned by the spectrum analyzer, as shown in Fig. 8, is continuously increasing from left to right at the rate of approximately 12 Hz/cycle. The pictured decrease in the magnitude of the capacitance changes at the higher frequencies was characteristic of all systems examined. Except for amplitude scaling, beds contained in the 2.54- and 3.18-cm tubes behaved identically.

Capacitance changes in this frequency range probably are a consequence of correspondingly short-lived changes in the configurations of particle clusters and in particle contact numbers. Such fluctuations at the particulate level are the result of particulate motion. For this reason, it is expected that useful information can be obtained by examining this frequency range over various shaking phase intervals. With the gating technique previously described, the relative magnitude of capacitance changes were analyzed as a function of frequency over various segments of the shaking cycle. Figure 9 shows spectra of 0.397-cm particles, at a

shaking amplitude of 0.442 cm, over two different 36° phase intervals, corresponding to periods of increasing bed expansion and of maximum bed expansion.

Two features of such spectra are worthy of note. As a bed expands, a given particle velocity distribution can be expected to result in increasingly lower frequency signals as interparticulate distances increase. The converse, of course, occurs during bed contraction. Thus, relative shifts in intensity *versus* frequency result from changes in bed density alone. The overall or average changes in intensity of these spectra are indicative of the relative intensities of the particulate motions they reflect and provide a relative measure of particulate kinetic energy.

CONCLUSIONS

It is generally recognized that the principal factors governing the rates of free-flowing solids mixing and segregation and their underlying mechanisms are the degree of bed dilation and the velocity distribution of the component particles (15). In many solids mixing or conveying operations, particle motion and bed dilation are strongly coupled and are the inseparable consequences of vibration and/or shear. The mechanisms by which both mixing and segregation occur under these forms of energy input are incompletely understood. Theories of these kinetic processes are commonly subjected to critical experimental verification based on their predictive capabilities; however, direct experimental evidence concerning other aspects of particle bed dynamics is often lacking.

The rates at which segregation and mixing occur within a vibrated bed are thought to vary considerably during each shaking cycle. Also, it is to be expected that these two processes do not necessarily increase and decrease in their intensities simultaneously or in phase. For these reasons, the kinetic behavior of mixing and segregation in vibrated particulate beds, as typically reported, reflects time-averaged rates that yield apparent rate constants representing minimum absolute values. Phase angles (Tables I and II) corresponding to various features of bed behavior can be used to estimate the time periods during each cycle when mixing and/or segregation primarily occur. Refinement of apparent rate constants to reflect more accurately their virtual values is, therefore, possible.

Data on the higher frequency fluctuations in capacitance that reflect movements of single particles or small clusters of particles may be applied to explain the magnitudes of the adjusted apparent rate constants. The details of such correlations will follow in subsequent reports. While the particles studied here have been idealized in size and shape, the methods discussed may be applied directly to any system of conducting particles and, excluding conductance measurements, can be arranged to apply to nonconducting systems.

APPENDIX

The gating circuit diagrammed in Fig. 5 was designed to pass signals having component frequencies ranging from dc to 50 kHz without distortion. Signals in this band were attenuated uniformly by the gate by a factor of 0.50. By adjusting the variable resistors at IC1 and IC2, the gate could be set to open, following the trigger pulse, after time delays of up to 60 msec. The variable resistor at IC3 permits adjusting the "open" phase of the gate for 2–30 msec.

Integrated circuits, IC1, IC2, and IC3, are type SN74121 monostable multivibrators and the high current switches, Q1 and Q2, are type 2N3642. A list of other components and power requirements as coded in Fig. 5 follows: A, 5-v dc supply; B, 12 kohm; C, 2 kohm; D, 35 kohm; E, 100 kohm (matched); F, 590 ohm; G, 39 kohm; H, 150 kohm; J, 2 μF; K, 1 μF; L, 10 μF; M, 100 pF; R, IN6424; S, IN457; and T, −4.5-v dc supply.

REFERENCES

(1) J. L. Olsen and E. G. Rippie, *J. Pharm. Sci.*, **53,** 147 (1964).

(2) E. G. Rippie, J. L. Olsen, and M. D. Faiman, *ibid.*, **53,** 1360 (1964).

(3) M. D. Faiman and E. G. Rippie, *ibid.*, **54,** 719 (1965).

(4) E. G. Rippie, M. D. Faiman, and M. K. Pramoda, *ibid.*, **56,** 1523 (1967).

(5) J. C. Anderson, "Dielectrics," Chapman and Hall, London, England, 1964.

(6) "High Frequency Dielectric Measurement," J. Chamberlain and G. W. Chantry, Eds., I. P. C. Science and Technology Press, Surrey, England, 1973, pp. 12, 28, 140.

(7) J. M. Dotson, J. H. Holden, C. B. Seibert, H. P. Simons, and L. D. Schmidt, *Chem. Eng.*, **56,** 129 (1949).

(8) P. J. Bakker and P. M. Heertjes, *Br. Chem. Eng.*, **3,** 240 (1958).

(9) D. Geldart and J. R. Kelsey, *Powder Technol.*, **6,** 45 (1972).

(10) V. A. Suprynowicz, "Introduction to Electronics for Students of Biology, Chemistry, and Medicine," Addison-Wesley, Reading, Mass., 1966, pp. 91, 316.

(11) L. K. H. van Beek, *Prog. Dielectr.*, **7,** 105 (1967).

(12) A. B. Carlson, "Communications Systems," 2nd ed., McGraw-Hill, New York, N.Y., 1975, p. 220.

(13) H. Takahashi, A. Suzuki, and T. Tanaka, *Powder Technol.*, **2,** 65 (1969).

(14) W. A. Gray and G. T. Rhodes, *ibid.*, **6,** 271 (1972).

(15) E. G. Rippie, in "The Theory and Practice of Industrial Pharmacy," 2nd ed., L. Lachman, H. A. Lieberman, and J. L. Kanig, Eds., Lea & Febiger, Philadelphia, Pa., 1976, pp. 498–500.

ACKNOWLEDGMENTS

Presented in part at the Basic Pharmaceutics Section, APhA Academy of Pharmaceutical Sciences, Atlanta meeting, November 1975.